

Isospin and symmetry energy study in nuclear EOS

TIAN WenDong^{1*}, MA YuGang¹, CAI XiangZhou¹, FANG DeQing¹, WANG HongWei¹
& WU HongLi^{1,2}

¹ Shanghai Institute of Applied Physics, Chinese Academy of Sciences, Shanghai 201800, China;

² Graduate School of University of Science and Technology of China, Hefei 230026, China

Received January 18, 2011; accepted April 21, 2011; published online July 27, 2011

This paper summarizes the isoscaling and isospin related studies in asymmetry nuclear reactions by different dynamic and statistical models. Isospin dependent quantum molecular dynamics model (IQMD) and lattice gas model (LGM) are used to study the isoscaling properties and isoscaling parameters dependence on incident energies, impact parameters, temperature and other parameters. In the LGM model, the signal of phase transition has been found in free neutron (proton) chemical potential difference $\Delta\mu_n$ or $\Delta\mu_p$ as a function of temperature, or in free neutron and proton chemical potential difference $\Delta\mu_n - \Delta\mu_p$. Density dependence of symmetry energy coefficient $C_{\text{sym}}(\rho/\rho_0)$ is also studied in the frame of LGM, with the potential parameters which can reproduce the nuclear ground state property, soft density dependence of symmetry energy is deduced from the simulation results. Giant dipole resonance (GDR) induced by isospin asymmetry in entrance channel is also studied via IQMD model, and the dynamic dipole resonance shows isospin sensitivity on the isospin asymmetry of entrance channel and symmetry energy of the nuclear equation of state (EOS). GDR can also be regarded as a possible isospin sensitive signature.

nuclear EOS, isospin, isoscaling, density, giant dipole resonance

PACS: 24.10.Pa, 24.30.Cz, 25.70.-z, 25.70.Ef

1 Introduction

The EOS of isospin asymmetric nuclear matter is a longstanding problem in both nuclear physics and astrophysics, and has received much attention in the past. The development of radioactive beam facilities around the world during the last decades, making it possible to experimentally study the properties of nuclear matter or nuclei under the extreme condition of large isospin asymmetry in terrestrial laboratories, and there has been a surge of research activities on this problem [1]. The one main goal of isospin physics is to determine the isospin dependence of the in-medium nuclear effective interactions and the equation of state (EOS) of isospin asymmetric nuclear matter or finite nuclei, particularly its isospin-dependent term, i.e., the density de-

pendence of the nuclear symmetry energy. Knowledge of nuclear symmetry energy is essential for understanding not only many problems in nuclear physics, such as the dynamics of heavy-ion collisions induced by radioactive beams and the structure of exotic nuclei, but also a number of important issues in astrophysics, such as the supernova simulation and neutron stars models, which require inputs for the nuclear equation of state at extreme values of density and asymmetry [2,3]. Impressive progress has been made both experimentally and theoretically, and a number of earlier reviews on isospin physics with heavy-ion reactions can be found in refs. [4–6].

Symmetry energy can be extracted from heavy-ion collision, and one sensitive observable of the symmetry energy is the fragment isotopic composition investigated via the isoscaling approach, which was first proposed in multifragmentation [7–10], then verified in a variety of reac-

*Corresponding author (email: tianwendong@sinap.ac.cn)

tions and theoretical studies [11–26].

The isoscaling law, which means that the ratio of isotope yields $R_{21}(N, Z) = Y_2(N, Z)/Y_1(N, Z)$, from two similar reactions, denoted as reactions 1 and 2, different only in their isospin asymmetry, is found to exhibit an exponential relationship as a function of the neutron number N and proton number Z [8–10], i. e.

$$R_{21}(N, Z) = \frac{Y_2(N, Z)}{Y_1(N, Z)} = C \exp(\alpha N + \beta Z), \quad (1)$$

where $Y_2(N, Z)$ and $Y_1(N, Z)$ are fragment yields from the neutron-rich and neutron-deficient reactions, respectively, C is an overall normalization factor, α and β are fitted parameters. The isoscaling parameter α is related to the symmetry energy coefficient C_{sym} of EOS in microcanonical and canonical frames by the following relation [8–10]:

$$\alpha = \frac{4C_{\text{sym}}}{T} \left[\left(\frac{Z}{A} \right)_2^2 - \left(\frac{Z}{A} \right)_1^2 \right], \quad (2)$$

where $(Z/A)_1$ and $(Z/A)_2$ are the charge and mass numbers of the sources from the two systems, and T is their temperature.

Determining the density dependence of the symmetry energy, $E_{\text{sym}}(\rho)$, becomes one of the main goals in nuclear physics at present and in the near future, and has been stimulated by many theoretical studies in experiments. Heavy ion collisions (HIC) with neutron-rich nuclei provide a unique opportunity to obtain the information on the density dependence of the symmetry energy in laboratories because a large extent of density can be formed during the HIC. Many useful observables from HIC, such as isoscaling, isospin diffusion [27–29], neutron to proton yield ratios and its flow at intermediate heavy ion collisions, have been proposed.

GDR is a collective vibration of protons against neutrons with a dipole spatial pattern that starts with the overlap of two nuclei in many reactions [30,31]. Some efforts have been made to study the dipole resonance formed during the fusion and incomplete fusion in N/Z asymmetry heavy ion reactions, so it could be a good probe for the symmetry term in the EOS [32].

2 Isoscaling property with IQMD and LGM

The mean field involved in the present IQMD model is given by $U(\rho) = U^{\text{Sky}} + U^{\text{Coul}} + U^{\text{Sym}}$, with U^{Sky} , U^{Coul} and U^{Sym} representing the skyrme potential, the Coulomb potential and symmetry potential, respectively [20]. The skyrme potential is $U^{\text{Sky}} = \alpha(\rho/\rho_0) + \beta(\rho/\rho_0)^\gamma$, where $\rho_0 = 0.16 \text{ fm}^{-3}$ is the nuclear saturate density. We take the parameters $\alpha = -356 \text{ MeV}$, $\beta = 303 \text{ MeV}$, and $\gamma = 7/6$ as a

soft EOS, $\alpha = -124 \text{ MeV}$, $\beta = 70.5 \text{ MeV}$, and $\gamma = 2$ as a hard EOS[33]. The symmetry potential is obtained by

$$U^{\text{sym}} = \frac{C_{\text{sym}}}{2\rho_0} \sum_{i \neq j} \tau_{iz} \tau_{jz} \frac{1}{(4\pi L)^{3/2}} \exp\left(-\frac{(r_i - r_j)^2}{4L}\right) \quad (3)$$

with C_{sym} the symmetry energy strength, τ_z being the z th component of the isospin degree of freedom, which equals 1 or -1 for neutrons or protons, respectively.

Simulation was performed for collisions $^{40}\text{Ca}+^{40}\text{Ca}$ and $^{48}\text{Ca}+^{48}\text{Ca}$ systems with impact parameter $b=1$ at several different incident energies $E/A=25, 35, 50, 70 \text{ MeV}$ [20]. Figure 1 shows the isoscaling parameter α and β dependence on incident energy. Isoscaling parameters are suppressed by the increase of incident energy, i.e., low incident energy makes the isoscaling phenomena more clear. Since high incident energy induces the collision more violently and isospin evolution becomes faster and deeper, then mere the isospin difference in two isospin different collisions. However too lower incident energy means few fragments emitted, results in difficult to collect enough isotope yields, especially the isotopes far from the stable line. Isoscaling parameters are connected with the temperature by $\alpha = \Delta\mu_n/T$ and $\beta = \Delta\mu_p/T$, where $\Delta\mu_n$ and $\Delta\mu_p$ are free neutron and proton chemical potential difference in two systems respectively, T is the system temperature. Normally Higher incident energy can produce higher system temperature T , therefore reduce the isoscaling parameters.

In Figure 2 the relation of isoscaling parameters α and $|\beta|$ with the impact parameter b is shown for collisions $^{40}\text{Ca}+^{40}\text{Ca}$ and $^{48}\text{Ca}+^{48}\text{Ca}$ at incident energy $35 \text{ MeV}/A$. The α and $|\beta|$ values raise with the increasing of impact parameter b . As we have discussed, the reactions become more violent from peripheral to central collision in the same incident energy case, more excitation energy can be achieved in the central collision, and system temperature T , which is

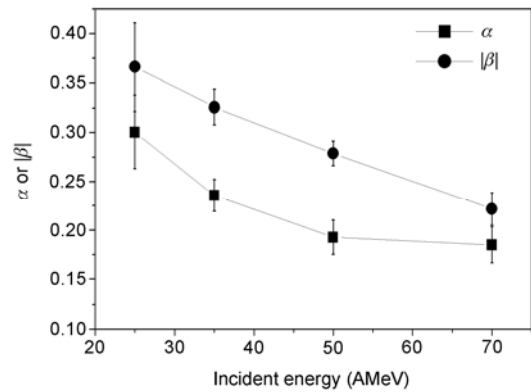


Figure 1 The variance of isoscaling parameters α and β with the incident energies for central collisions $^{40}\text{Ca}+^{40}\text{Ca}$ and $^{48}\text{Ca}+^{48}\text{Ca}$.

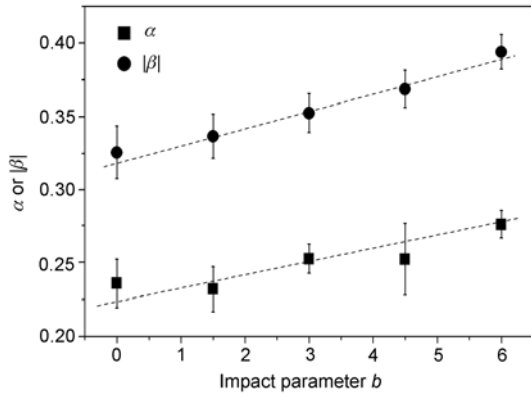


Figure 2 Relation of isoscaling parameters α and β with the impact parameter b , at incident energy 35 AMeV for collisions $^{40}\text{Ca}+^{40}\text{Ca}$ and $^{48}\text{Ca}+^{48}\text{Ca}$.

directly connected with the excitation energy. The higher temperature in the central collision reduces the isoscaling parameters α and $|\beta|$, and this dependence also indicates that large isospin effect can be observed in peripheral collisions than in central collisions.

The lattice gas model was developed to describe the liquid-gas phase transition for an atomic system by Lee and Yang [34]. The same model has already been applied to nuclear physics for isospin symmetrical systems in the grand-canonical ensemble [35–37] with a sampling of the canonical ensemble [38–41] and also for isospin asymmetrical nuclear matter in the mean field approximation [42].

In the lattice gas model, $A(N+Z)$ nucleons with an occupation number s which is defined $s=1$ (-1) for a proton (neutron) or $s=0$ for a vacancy are placed on the L sites of lattice. Nucleons in the nearest-neighboring sites interact with an energy $\varepsilon_{s_i s_j}$. The Hamiltonian is written as:

$$E = \sum_{i=1}^A \frac{p_i^2}{2m} - \sum_{i<j} \varepsilon_{s_i s_j} s_i s_j. \quad (4)$$

In order to investigate the symmetrical term of the nuclear potential in this model, we use two sets of parameters: one is an attractive potential constant $\varepsilon_{s_i s_j}$ between neutrons and protons but no interaction between like nucleon, i.e. proton and proton or neutron and neutron—namely:

$$\varepsilon_{nn} = \varepsilon_{pp} = 0 \text{ MeV}, \quad \varepsilon_{pn} = -5.33 \text{ MeV}, \quad (5)$$

This potential results in an asymmetrical potential among different kinds of nucleons; hence it is an isospin-dependent potential, and it is called isoLGM. And another interaction set

$$\varepsilon_{nn} = \varepsilon_{pp} = \varepsilon_{pn} = -5.33 \text{ MeV} \quad (6)$$

is called noisoLGM.

Small-size nuclei with $A=36$ as emission sources are chosen [17]. Four isotonic sources—namely, ^{36}Ca , ^{36}Ar ,

^{36}S , and ^{36}Si —corresponding to $N/Z=0.8, 1.0, 1.25,$ and 1.57 , respectively, are simulated. In all cases, the freeze out density ρ_f is chosen to be $0.563 \rho_0$, which corresponds to a 4^3 cubic lattice. Here, 10000 events are simulated for each T which ensures good statistics for the results.

Figure 3 shows the extracted α and β versus Z or N . Obviously, α and β keep the same value in the wide Z or N range and their absolute values are almost the same, which is due to the absence of a Coulomb interaction in the lattice gas model.

Figure 4 shows the temperature dependence of the absolute values of isoscaling parameters α and β . In which the scattering points are the calculation results with asymmetrical nucleon-nucleon potential, and the lines are the results with noisoLGM interaction. The decreasing dependence of isoscaling parameters α and $|\beta|$ on temperature can be seen in the isoLGM results, which indicates that the isospin dependence of the fragment yields becomes weak with the increase of temperature. This dependence is in accord with the result of IQMD in Figure 1, i.e., the decrease of isoscaling parameter on the incident energy.

Considering the above mentioned relation between isos-

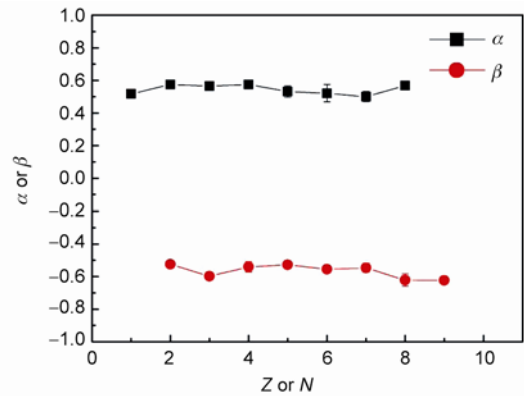


Figure 3 (Color online) Isoscaling parameters α and β extracted in fixed Z and N , respectively.

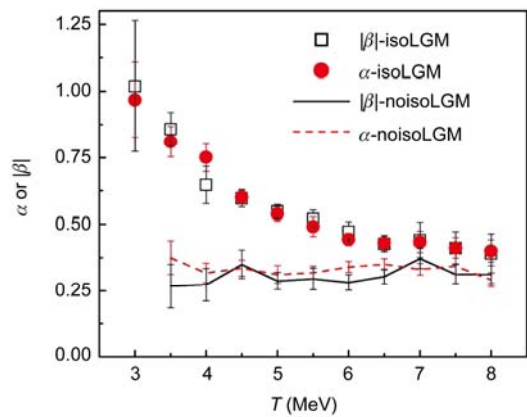


Figure 4 (Color online) The absolute value of the isoscaling parameters α and β as a function of T from the yield ratios with sources of ^{36}S and ^{36}Ca .

caling parameters and the free neutron (proton) chemical potential difference equation $\alpha=\Delta\mu_n/T$ and $\beta=\Delta\mu_p/T$, we can deduce the free neutron or proton chemical potential difference of the sources, as a function of the source temperature T , as shown in Figure 5(a). Within the error bars, it looks like that $\Delta\mu_n$ and $\Delta\mu_p$ keep constant in the case of an asymmetrical potential. However, a slight and wide valley can also be identified around $T=5$ MeV as well as a slight kink showing in the SMM model for Sn systems [43]. This valley may be related to the liquid gas phase change for a similar system around 5 MeV in the same model calculation as well as in the data [44]. This valley becomes obvious if we plot the values of $(\Delta\mu_n-\Delta\mu_p)/2$ as a function of temperature as suggested in ref. [43]. Figure 5(b) shows that a turning point seems to occur around 5 MeV.

Around this point, an apparent critical behavior has been observed in the disassembly of hot nuclei with $A=36$ in TAMU-NIMROD experimental data and model calculations [44] by a wide variety of observables [45,46]. This turning point of the difference between neutron and proton chemical potentials might give additional evidence of the chemical phase separation when the liquid-gas phase transition occurs.

3 Density dependence of symmetry energy nuclear EOS in the lattice gas model

In order to study the density dependence of isoscaling and symmetry energy, equilibrated source pairs are chosen with different system isospin asymmetry $N=Z$, and groups of the

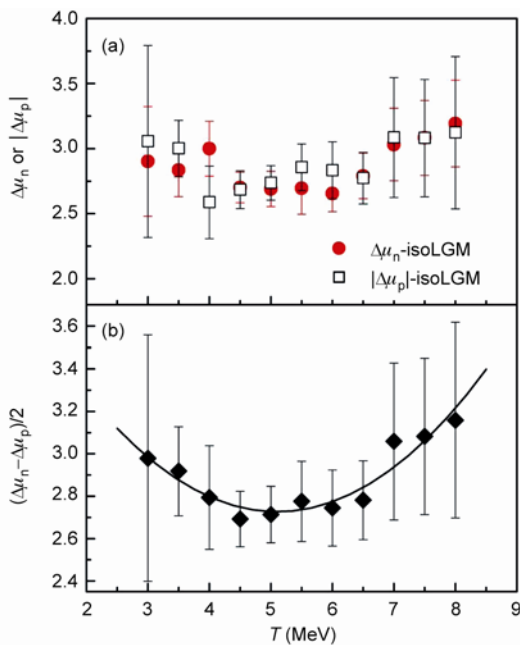


Figure 5 (Color online) (a) The absolute value of the difference of neutron and proton chemical potential ($\Delta\mu_n$ and $|\Delta\mu_p|$) as a function of T ; (b) $(\Delta\mu_n-\Delta\mu_p)/2$ as a function of temperature, and the line is the second polynomial fit.

source pairs have been used: $Z = 30$ with $A=60, 63, 66$ and 69 , respectively, corresponding to $N/Z=1, 1.1, 1.2$ and 1.3 . The freeze-out density ρ_f is chosen to be $0.48\rho_0, 0.28\rho_0, 0.18\rho_0, 0.12\rho_0$ and $0.08\rho_0$, in which $5^3, 6^3, 7^3, 8^3$ and 9^3 cubic lattice were used for $A=60$, respectively. However, slightly different ρ_f values are obtained for $A=63, 66$ and 69 due to their mass differences [47].

We perform calculations on sources with different isospin asymmetry for different densities at $T=3$ MeV. Figure 6(a) shows that α increases with the difference of the source isospin asymmetry. From eq. (1) the symmetry energy coefficient C_{sym} can be extracted from the isoscaling parameter α . The symmetry energy plays an important role in nuclear structure of the nuclei with large isospin asymmetry, and the study of the isoscaling parameters at different density can be used to probe the isospin dependent symmetry energy. Figure 6(b) shows that the deduced symmetry energy coefficient C_{sym} by eq. (1) is a function of freeze-out density at different temperature. By fitting the data point in Figure 6(b) with a form of function $C_{\text{sym}} = C_0(\rho/\rho_0)^\gamma$, we obtain the parameters $C_0=24$ MeV and $\gamma=0.59$. This value is in the range suggested by other models and the data [48], but a little softer than that in ref. [28].

4 The study of isospin asymmetry induced GDR by IQMD

The giant dipole moment in coordinator space $DR(t)$ and

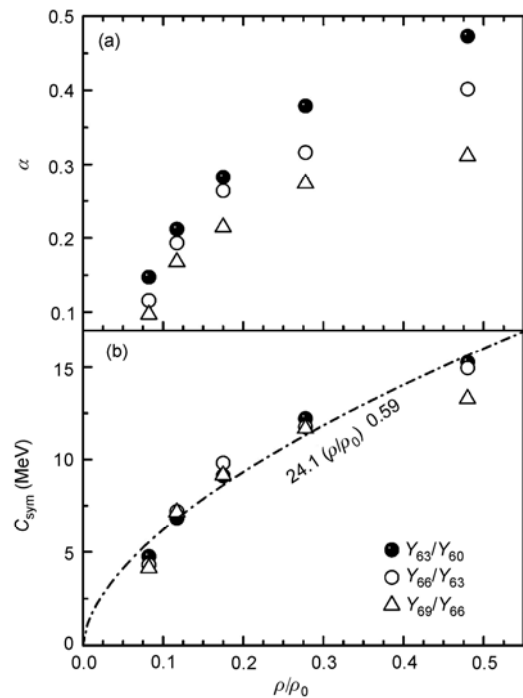


Figure 6 (a) Isoscaling parameters α as a function of density from different isospin asymmetry sources; (b) density dependence of the deduced symmetry energy coefficient from (a).

momentum space $DK(t)$ is written, respectively, as follows [31]:

$$DR(t) = \frac{NZ}{A} X(t) = \frac{NZ}{A} (R_Z - R_N), \quad (6)$$

where $X(t)$ is the distance between the centers of the mass of protons and neutrons, $R_Z = \sum_i x_i(p)$ and $R_N = \sum_i x_i(n)$ is the center of the mass of protons and neutrons, respectively, and

$$DK(t) = \frac{NZ}{A\hbar} \Pi(t) = \frac{NZ}{A\hbar} \left(\frac{P_p}{Z} - \frac{P_n}{N} \right) \quad (7)$$

is just the canonically conjugate momentum of the $DR(t)$, where $\Pi(t)$ denotes the relative momentum, with $P_n(P_p)$ centers of the mass in momentum space for neutrons and protons.

Here, $N=N_p+N_T$ and $Z=Z_p+Z_T$, and the suffix P (or T) marks projectile (or target). The initial dipole moment can be calculated by eq. (6):

$$\begin{aligned} DR(t=0) &= \frac{NZ}{A} (R_Z(t=0) - R_N(t=0)) \\ &= \frac{R_p + R_T}{A} Z_p Z_T \left[\left(\frac{N}{Z} \right)_T - \left(\frac{N}{Z} \right)_p \right] \end{aligned} \quad (8)$$

where R_p and R_T are the radii of the projectile and target, respectively.

Derived from the overall dipole moment $D(t)$, we can get the γ -ray emission probability for energy E [31,49]:

$$\frac{dP}{dE} = \frac{2}{3\pi} \frac{e^2}{E\hbar c} \left| \frac{d\bar{V}_k}{dt}(E) \right| \quad (9)$$

where dP/dE can be interpreted as the average number of γ ray emitted per energy unit, while $d\bar{V}_k/dt(E)$ is the Fourier transformation of the time derivation on the k th components x and z of \bar{V} .

Figure 7 shows the evolution of the giant dipole moment with time in coordinate space and momentum space for $^{40}\text{Ca}+^{48}\text{Ca}$ collision at 10 MeV/nucleon and $b=1$ fm. The periodical vibration in both coordinate and momentum space between protons and neutrons can be seen clearly, and it damps with the evolution time. The giant dipole moment attenuates rapidly after $t=400$ fm/c, illustrating a clear reduction of the collective behavior [50].

To determine the reliability of our calculation of dipole γ emission with the IQMD model, experimental data for the $^{40}\text{Ca}+^{48}\text{Ca}$ system [51] at $E_{\text{beam}}=10$ MeV/nucleon and $^{16}\text{O}+^{116}\text{Sn}$ system [52] at $E_{\text{beam}}=15.6$ MeV/nucleon are compared with our result in Figure 8. It should be noted that the experimental data on dynamical dipole emission here are obtained by taking away the statistical contribution (result of the statistical model calculation) from the measured

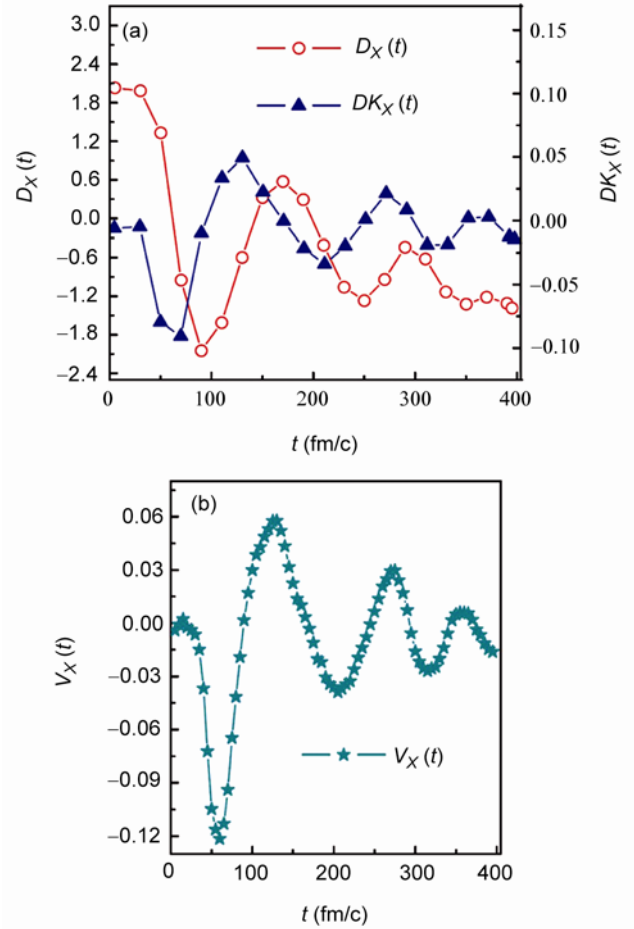


Figure 7 (Color online) (a) Evolution of the giant dipole moment with time in coordinate space $D_X(t)$ and momentum space $DK_X(t)$; (b) dynamical dipole mode $|V_X(t)|$.

spectrum. Both systems calculated here are carried out with soft Skyrme potential and impact parameters being a triangle distribution between 1 and 6 fm. The good agreement between the data and the IQMD calculation encourages us to make systematic calculation on dynamic GDR γ emission on isospin asymmetry effect.

The correlation between the dynamical dipole emission and the symmetry term of the EOS is investigated by changing the symmetry energy coefficient (C_{sym}). In the top panel in Figure 9, the spectrum of dynamic emission of the same system $^{40}\text{Ca}+^{48}\text{Ca}$ is reported, and the calculation is performed in the same situation except for the C_{sym} . We can clearly see an increased yield of γ rays for larger C_{sym} values.

As mentioned before, another interesting aspect of the GDR emission property is its dependence on the N/Z asymmetry of the reaction systems, which in fact is a direct result of eq. (8). This relationship is of most importance for its association with the symmetry term of the EOS. So by taking the charge and mass symmetry system $^{40}\text{Ca}+^{40}\text{Ca}$ as a reference system, the dynamic giant dipole resonance is not

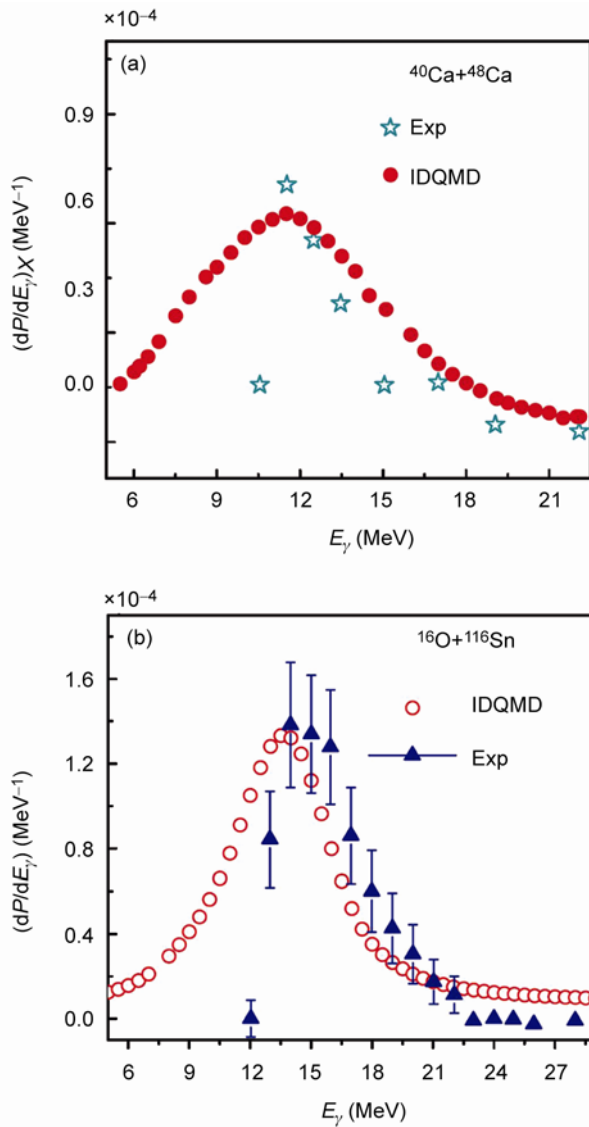


Figure 8 (a) Experimental data (stars) [51] together with IQMD calculation (solid circles) of the γ -ray spectrum of the $^{40}\text{Ca}+^{48}\text{Ca}$ system at 10 MeV/nucleon; (b) measured value of γ -ray yield for the $^{16}\text{O}+^{116}\text{Sn}$ system at 15.6 MeV/nucleon (filled triangles) [52] and our calculation results (open circles) under the same conditions.

expected because of small initial dipole moment in both coordinate and momentum space.

Calculations of dipole γ emission in N/Z asymmetry systems $^{40}\text{Ca}+^{48}\text{Ca}$ and $^{40}\text{Ca}+^{52}\text{Ca}$ are performed. In the bottom panel of Figure 9, we show the results for γ emission in the early 400 fm/c at $E_{\text{beam}}=10$ MeV/nucleon, with $b=4$ fm and soft EOS. In the inset, the ratio of γ yields are also shown, where the ratio between the $^{40}\text{Ca}+^{48}\text{Ca}$ and $^{40}\text{Ca}+^{40}\text{Ca}$ systems is shown by filled circles, and the ratio between $^{40}\text{Ca}+^{52}\text{Ca}$ and $^{40}\text{Ca}+^{40}\text{Ca}$ systems is denoted by open triangles. From the figure one find that the N/Z asymmetry systems $^{40}\text{Ca}+^{48}\text{Ca}$ ($N/Z=1.3$) and $^{40}\text{Ca}+^{52}\text{Ca}$ ($N/Z=1.2$) show a clear enhanced yield of the order of about 20% and 35%,

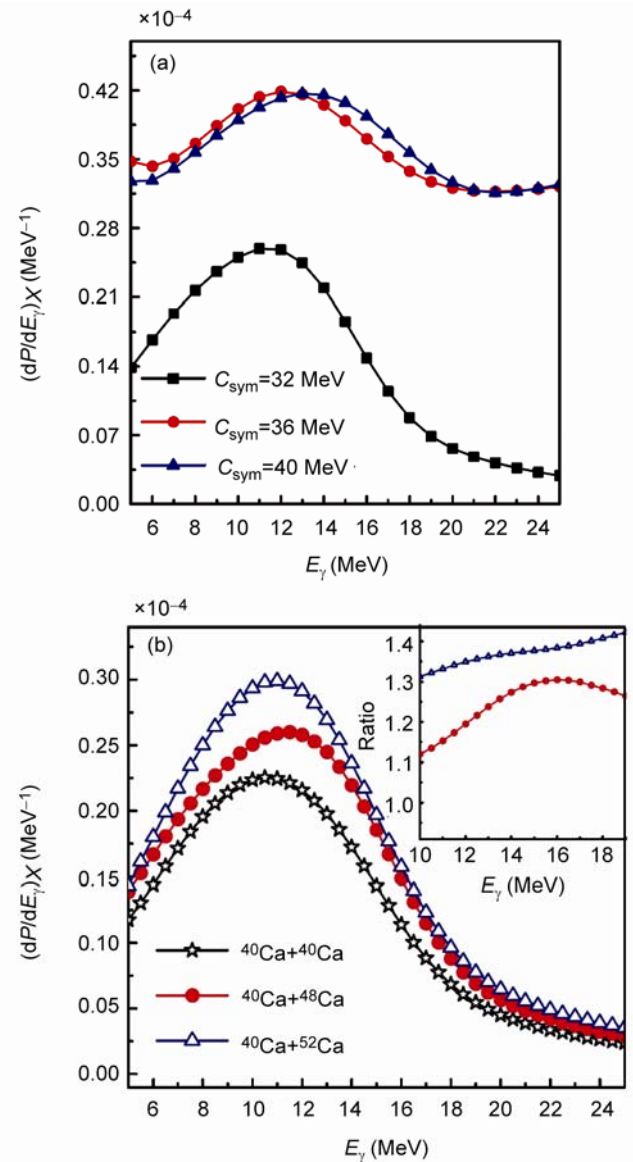


Figure 9 (a) Symmetry energy coefficient (C_{sym}) dependence of γ emission probability for the system $^{40}\text{Ca}+^{48}\text{Ca}$ at $E_{\text{beam}}=10$ MeV/nucleon and $b=4$ fm; (b) γ emission probability of systems $^{40}\text{Ca}+^{52}\text{Ca}$ and $^{40}\text{Ca}+^{48}\text{Ca}$ and reference system $^{40}\text{Ca}+^{40}\text{Ca}$ at $E_{\text{beam}}=10$ MeV/nucleon and $b=4$ fm with soft EOS ($C_{\text{sym}}=32$ MeV). Inset: Ratio of γ yields of systems with a ^{48}Ca target or ^{52}Ca target to those with a ^{40}Ca target.

with respect to the symmetry system $^{40}\text{Ca}+^{40}\text{Ca}$ ($N/Z=1.0$), consistent with the result in ref. [49] and references therein.

5 Conclusions

We have investigated the isoscaling properties by IQMD and isospin dependent LGM. In LGM model calculation, the possible phase transition signal has been proposed by the difference of free proton and neutron chemical potential difference $(\Delta\mu_n-\Delta\mu_p)/2$ as a function of temperature. Symmetry energy coefficient and density dependence of sym-

metry energy are also investigated through LGM model simulation, and soft density dependence of symmetry energy is obtained. We tried to observe the dynamic dipole γ emission from the isospin asymmetry nuclei induced reactions, and found that GDR γ emission is sensitive to the symmetry energy. This offers another method to probe the isospin degree in nuclear EOS.

Symmetry energy study in nuclear EOS with isospin asymmetry nuclei and nuclear matter is the critical research at present, for both exotic nuclei structure and reactions induced by isospin asymmetry nuclei. We have paid much efforts to look for the probes of isospin degree. Isoscaling is one of the probes that can directly connect symmetry energy coefficient with the experimental observable. Many measurements and calculations have been devoted to this subject, and have got considerable achievements. Now, the constraint of the symmetry energy dependence on density is the essential work, and more observables are needed to give further information of the symmetry energy term in nuclear EOS and isospin degree in nuclear physics.

This work was supported by the National Natural Science Foundation of China (Grant Nos. 10875160, 10979074 and 11035009), and the Major State Basic Research Development Program in China (Grant No. 2007CB815004).

- 1 Li B A, Schröder W. *Isospin Physics in Heavy-Ion Collisions at Intermediate Energies*. New York: Nova Science Publishers, Inc., 2001
- 2 Lattimer J M, Pethick C J, Prakash M, et al. Direct URCA process in neutron stars. *Phys Rev Lett*, 1991, 66: 2701–2704
- 3 Lattimer J M, Prakash M. Nuclear matter and its role in supernovae, neutron stars and compact object binary mergers. *Phys Rep*, 2000, 333: 121–146
- 4 Baran V, Colonna M, Greco V, et al. Reaction dynamics with exotic nuclei. *Phys Rep*, 2005, 410: 335–475
- 5 Steiner A W, Prakash M, Lattimer J M, et al. Isospin asymmetry in nuclei and neutron stars. *Phys Rep*, 2005, 411: 325–375
- 6 Li B A, Chen L W, Ko C M. Recent progress and new challenges in isospin physics with heavy-ion reactions. *Phys Rep*, 2008, 464: 113–282
- 7 Xu H S, Tsang M B, Liu T X, et al. Isospin fractionation in nuclear multifragmentation. *Phys Rev Lett*, 2000, 85: 716–719
- 8 Tsang M B, Friedman W A, Gelbke C K, et al. Isotopic scaling in nuclear reactions. *Phys Rev Lett*, 2000, 86: 5023–5026
- 9 Tsang M B, Friedman W A, Gelbke C K, et al. Conditions for isoscaling in nuclear reactions. *Phys Rev C*, 2001, 64: 041603(R)
- 10 Tsang M B, Gelbke C K, Liu X D, et al. Isoscaling in statistical models. *Phys Rev C*, 2001, 64: 054615
- 11 Botvina A S, Lozhkin O V, Trautmann W. Isoscaling in light-ion induced reactions and its statistical interpretation. *Phys Rev C*, 2002, 65: 044610
- 12 Shetty D V, Yennello S J, Martin E, et al. Energy dependence of the isotopic composition in nuclear multifragmentation. *Phys Rev C*, 2003, 68: 021602(R)
- 13 Souliotis G A, Shetty D V, Veselsky M, et al. Isotopic scaling of heavy projectile residues from the collisions of 25 MeV/nucleon ^{86}Kr with ^{124}Sn , ^{112}Sn and ^{64}Ni , ^{58}Ni . *Phys Rev C*, 2003, 68: 024605
- 14 Ono A, Danielewicz P, Friedman W A, et al. Isospin fractionation and isoscaling in dynamical simulations of nuclear collisions. *Phys Rev C*, 2003, 68: 051601
- 15 Friedman W A. Isotopic yields and isoscaling in fission. *Phys Rev C*, 2004, 69: 031601(R)
- 16 Veselsky M, Souliotis G A, Yennello S J. Isoscaling in peripheral nuclear collisions around the Fermi energy and a signal of chemical separation from its excitation energy dependence. *Phys Rev C*, 2004, 69: 031602(R)
- 17 Ma Y G, Wang K, Wei Y B, et al. Isoscaling in the lattice gas model. *Phys Rev C* 2004, 69: 064610
- 18 Shetty D V, Yennello S J, Botvina A S, et al. Symmetry energy and the isospin dependent equation of state. *Phys Rev C*, 2004, 70: 011601(R)
- 19 Geraci E, Brunoa M, D'Agostino M, et al. Isoscaling in central $^{124}\text{Sn} + ^{64}\text{Ni}$, $^{112}\text{Sn} + ^{58}\text{Ni}$ collisions at 35 A MeV. *Nucl Phys A*, 2004, 732: 173–201
- 20 Tian W D, Ma Y G, Cai X Z, et al. Isoscaling behavior in the isospin-dependent quantum molecular dynamics model. *Chin Phys Lett*, 2005, 22: 306–309
- 21 Raduta Ad R. Microcanonical studies on isoscaling. *Eur Phys J A* 2005, 24: 85–92
- 22 Ma Y G, Wang K, Cai X Z, et al. Isoscaling behavior in fission dynamics. *Phys Rev C*, 2005, 72: 064603
- 23 Dorso C O, Escudero C R, Ison M, et al. Dynamical aspects of isoscaling. *Phys Rev C*, 2006, 73: 044601
- 24 Tian W D, Ma Y G, Cai X Z, et al. Isospin effect in statistical sequential decay. *Phys Rev C*, 2007, 76: 024607
- 25 Galanopoulos S, Souliotis G A, Keksis A L, et al. Isoscaling of mass $A \approx 40$ reconstructed quasiprojectiles from collisions in the Fermi energy regime. *Nucl Phys A*, 2010, 837: 145–162
- 26 Chen Z, Kowalski S, Huang M, et al. Isoscaling and the symmetry energy in the multifragmentation regime of heavy-ion collisions. *Phys Rev C*, 2010, 81: 064613
- 27 Tsang M B, Liu T X, Shi L, et al. Isospin diffusion and the nuclear symmetry energy in heavy ion reactions. *Phys Rev Lett*, 2004, 92: 062701
- 28 Chen L W, Ko C M, Li B A, et al. Determination of the stiffness of the nuclear symmetry energy from isospin diffusion. *Phys Rev Lett*, 2005, 94: 032701
- 29 Li B A, Chen L W. Nucleon-nucleon cross sections in neutron-rich matter and isospin transport in heavy-ion reactions at intermediate energies. *Phys Rev C*, 2005, 72: 064611
- 30 Snover K A. Giant resonances in excited nuclei. *Annu Rev Nucl Part Sci*, 1986, 36: 545–603
- 31 Baran V, Cabibbo M, Colonna M, et al. The dynamical dipole mode in dissipative heavy-ion collisions. *Nucl Phys A*, 2001, 679: 373–392
- 32 Baran V, Colonna M, Greco V, et al. Reaction dynamics with exotic nuclei. *Phys Rep*, 2005, 410: 335–466
- 33 Aichelin J. “Quantum” molecular dynamics—a dynamical microscopic n-body approach to investigate fragment formation and the nuclear equation of state in heavy ion collisions. *Phys Rep*, 1991, 202: 233–360
- 34 Lee T D, Yang C N. Statistical theory of equations of state and phase transitions. II. Lattice gas and ising model. *Phys Rev*, 1952, 87: 410–419
- 35 Biro T S, Knoll J, Richert J, et al. Percolation in finite space: A picture of nuclear fragmentation? *Nucl Phys A*, 1986, 459: 692–710
- 36 Samaddar S K, Richert J. Effect of short- and long-range interactions on cluster multiplicities in finite excited systems. *Phys Lett B*, 1989, 218: 381–385
- 37 Carmona J M, Richert J, Tarancón A. A model for nuclear matter fragmentation: Phase diagram and cluster distributions. *Nucl Phys A*, 1998, 643: 115–134
- 38 Müller W F J. Canonical sampling of a lattice gas. *Phys Rev C*, 1997, 56: 2873–2874

- 39 Campi X, Krivine H. Clustering in supercritical nuclear matter: A lattice-gas approach. *Nucl Phys A*, 1997, 620: 46–54
- 40 Ma Y G, Su Q M, Shen W Q, et al. Isospin effects of critical behavior in lattice gas model. *Chin Phys Lett*, 1999, 16: 256–258
- 41 Ma Y G, Su Q M, Shen W Q, et al. Isospin influences on particle emission and critical phenomena in nuclear dissociation. *Phys Rev C*, 1999, 60: 024607
- 42 Ray S, Shamanna J, Kuo T T S. Isospin lattice gas model and liquid-gas phase transition in asymmetric nuclear matter. *Phys Lett B*, 1997, 392: 7–12
- 43 Botvina A S, Lozhkin O V, Trautmann W. Isoscaling in light-ion induced reactions and its statistical interpretation. *Phys Rev C*, 2002, 65: 044610
- 44 Ma Y G, Wada R, Hagel K, et al. Evidence of critical behavior in the disassembly of nuclei with $A \sim 36$. *Phys Rev C*, 2004, 69: 031604(R)
- 45 Ma Y G. Application of information theory in nuclear liquid gas phase transition. *Phys Rev Lett*, 1999, 83: 3617–3620
- 46 Ma Y G. Zpif's law in the liquid gas phase transition of nuclei. *Eur Phys J A*, 1999, 6: 367–371
- 47 Su Q M, Ma Y G, Tian W D, et al. Density and symmetric potential dependences of isoscaling behaviour in the lattice gas model. *Chin Phys Lett*, 2008, 25: 2000–2003
- 48 Shetty D V, Yennello S J, Souliotis G A. Density dependence of the symmetry energy and the nuclear equation of state: A dynamical and statistical model perspective. *Phys Rev C*, 2007, 76: 024606
- 49 Papa M, Bonanno A, Amorini F, et al. Coherent and incoherent giant dipole resonance γ -ray emission induced by heavy ion collisions: Study of the $^{40}\text{Ca}+^{48}\text{Ca}$ system by means of the constrained molecular dynamics model. *Phys Rev C*, 2003, 68: 034606
- 50 Wu H L, Tian W D, Ma Y G, et al. Dynamical dipole γ radiation in heavy-ion collisions on the basis of a quantum molecular dynamics model. *Phys Rev C*, 2010, 81: 047602
- 51 Papa M, Tian W D, Giuliani G, et al. Pre-equilibrium γ -ray emission induced in the $^{40}\text{Ca}+^{48}\text{Ca}$ system at 10 MeV/nucleon and isospin equilibration processes. *Phys Rev C*, 2005, 72: 064608
- 52 Corsi A, Wieland O, Kravchuk V L, et al. Excitation of the dynamical dipole in the charge asymmetric reaction $^{16}\text{O} + ^{116}\text{Sn}$. *Phys Lett B*, 2009, 679: 197–202